

Article

# Revealing Chaos Synchronization Below the Threshold in Coupled Mackey–Glass Systems

Marat Akhmet <sup>1,\*</sup>, Kağan Başkan <sup>2</sup> and Cihan Yeşil <sup>2</sup><sup>1</sup> Department of Mathematics, Middle East Technical University, Dumlupınar Boulevard, 06800 Ankara, Turkey<sup>2</sup> Department of Physics, Middle East Technical University, Dumlupınar Boulevard, 06800 Ankara, Turkey; kagan.baskan@metu.edu.tr (K.B.); cihan.yesil@metu.edu.tr (C.Y.)

\* Correspondence: marat@metu.edu.tr; Tel.: +90-312-210-53-55

**Abstract:** This study presents a novel concept in chaos synchronization, delta synchronization of chaos, which reveals the presence of chaotic models evolving in unison even in the absence of generalized synchronization. Building upon an analysis of unpredictability in Poincaré chaos, we apply this approach to unilaterally coupled time-delay Mackey–Glass models. The main novelty of our investigation lies in unveiling the synchronization phenomenon for a coupling constant below the synchronization threshold, an unattainable domain for conservative methods. Furthermore, we rigorously examine the coexistence of generalized synchronization and complete synchronization of unpredictability, which is a special case of delta synchronization, above the threshold. Therefore, the threshold is no longer a requirement for the synchronization of chaos in view of the present results. Additionally, transitions to fully chaotic regimes are demonstrated via return maps, phase portraits, and a bifurcation diagram. The findings are substantiated by tables and novel numerical characteristics.

**Keywords:** synchronization; delta synchronization; unpredictability; Poincaré chaos; Mackey–Glass system

**MSC:** 65P20; 37M05; 37M10; 37N30



**Citation:** Akhmet, M.; Başkan, K.; Yeşil, C. Revealing Chaos

Synchronization Below the Threshold in Coupled Mackey–Glass Systems. *Mathematics* **2023**, *11*, 3197. <https://doi.org/10.3390/math11143197>

Academic Editors: João Cabral, Daniele Fournier-Prunaret and José Leonel Linhares da Rocha

Received: 19 June 2023  
Revised: 11 July 2023  
Accepted: 18 July 2023  
Published: 21 July 2023



**Copyright:** © 2023 by the authors. Licensee MDPI, Basel, Switzerland. This article is an open access article distributed under the terms and conditions of the Creative Commons Attribution (CC BY) license (<https://creativecommons.org/licenses/by/4.0/>).

## 1. Introduction

Various types of chaos synchronization have been investigated and applied to numerous dynamical models concerning different areas of science [1–14]. The phenomenon is examined using several methods, which are identical synchronization, generalized synchronization, phase synchronization, anticipated synchronization, lag synchronization, and amplitude envelope synchronization [15,16]. We have introduced a new method to detect chaos synchronization with the name *delta synchronization of chaos* (DSC) [17,18]. The implementation of DSC into electronic systems has shown that it is able to reveal chaos synchronization even if the systems do not reveal the generalized synchronization [17,18].

The primary condition for this novel numerical method is the existence of unpredictability in drive and response systems. The concept of unpredictable motion investigates the time sequences at the moments of convergence to the initial point and separation from the initial trajectory [19–21]. The former and the latter are called the sequence of convergence and sequence of separation, respectively. The coexistence of the sequences shows that the system has necessary Poincaré chaos [19–21]. Chaos was initiated in the Poincaré recurrence theorem [22], which states that certain dynamical systems in continuous time will, after a sufficiently long but finite time, return to a state arbitrarily close to their initial state. Individual motions of the dynamics are Poisson stable. The final version of the theorem was proved using methods of measure theory in [23]. The motions of Poincaré chaotic dynamics [19–21] are Poisson stable and additionally equipped with an unpredictability property. It is proved in Ref. [19] that the dynamics are sensitive, and consequently, all ingredients of chaos are present. It is of strong interest to reconsider the

recurrence theorem under the condition of unpredictability to make its connection with chaotic dynamics maximally clear.

The DSC aims to detect common sequences of convergence and separation between drive and response systems. If the sequence of convergence is finite and does not numerically converge to the initial point, the type of synchronization is called delta synchronization. In the case of complete convergence, it is called *complete synchronization of unpredictability*. In previous studies [17,18], the DSC method was successfully applied to gas discharge semiconductor systems, which involve ordinary and partial differential equations. In this study, we extend the application of the DSC method to delay differential equations. Furthermore, we encourage the exploration of synchronization analysis for chaotic systems using the DSC in other types of differential equations, including fractional differential equations. Recent studies demonstrated substantial advancements in synchronization analysis for nonlocal models [24], suggesting promising opportunities for further investigation through the application of the DSC.

The relationship between unpredictable motions and generalized synchronization was theoretically investigated in a recent study [25]. The paper proves that if the drive system has an unpredictable solution and generalized synchronization exists in the coupled system, then the response system must have an unpredictable solution. The papers [17,18] and the present study numerically support this argument. In one paper [25], unpredictability in the response system is approved through generalized synchronization, but it cannot be considered to be theoretical support for our research since the sufficient conditions of the paper are not valid for our case. However, the results of the paper confirm that our suggestions can initiate serious mathematical investigations. Another remarkable investigation of unpredictability was presented in paper [26], which increases the effectiveness of unpredictable motions. It is emphasized that the approach can be applied to chaos synchronization research.

Time-delay systems are crucial for chaos synchronization research, especially in secure communication [27–29]. The present study investigates the DSC in Mackey–Glass systems [30], which are first-order delay differential equations originally developed for modeling blood production. They are capable of generating chaotic behaviors for specific parameter regimes [30,31]. The electronic circuit implementation of models enables researchers to analyze the synchronization of chaos experimentally [32–34].

Unidirectionally coupled Mackey–Glass drive-response systems exhibit synchronization in chaotic regimes, which is characterized by specific thresholds [33,35–38]. Previous studies, such as Ref. [37], showed that coupled systems achieve generalized and complete synchronization only above a certain threshold. In this paper, we aim to investigate the synchronized behavior of the Mackey–Glass drive-response systems using the same parameters as in Ref. [37] on both sides of this threshold, employing the DSC method. Furthermore, Ref. [35] demonstrated the existence of synchronization when the coupling parameter exceeds a threshold, considering different delay times in the drive and response systems. Additionally, Ref. [36] analytically and numerically explored the relationship between synchronization thresholds and delay times. Additionally, in Ref. [38], synchronization regimes and stability conditions of two linearly and nonlinearly coupled Mackey–Glass systems were analyzed.

The main motivation of this paper is to demonstrate the occurrence of synchronous chaotic behavior in drive-response Mackey–Glass systems within regimes that lack generalized synchronization. The specific threshold for synchronization varies with different parameters of the Mackey–Glass models. Previous research conducted in the field consistently reveals that synchronization is present on one side of the threshold while absent on the other [33,35–38]. Furthermore, studies have indicated that generalized and complete synchronization coexists on the same side of the threshold [35,37]. Our investigation reveals that synchronization can occur and be detected by the DSC below the threshold, where no synchronization was observed before. Additionally, in the region where generalized synchronization exists, we observe the coexistence of complete synchronization of unpre-

dictability, a special case of the DSC. Similar results obtained in Refs. [17,18] reinforce the significance of our synchronization research and provide a solid foundation for the DSC method.

The numerical characteristics of the method are defined to support the argument. In this investigation, the synchronization of unpredictability proves the synchronization of chaos. We believe that revealing the synchronous dynamics, where the region is known as asynchronous for the coupled system previously, can also contribute to the secure communication research field. Moreover, the coexistence of complete synchronization of unpredictability and generalized synchronization, above the threshold, is observed.

The organization of the paper is as follows. A brief description of methods is presented in *Preliminaries*. Transition to the chaotic regime in the model under research is carefully examined in Section 3. The main results of the present study; the unpredictability, complete synchronization of unpredictability, delta synchronization, and their comparison with the generalized synchronization in the coupled Mackey–Glass models are in Section 4. Finally, *Conclusion* emphasizes the discoveries of the study.

## 2. Preliminaries

Unpredictability analysis is used to detect the chaotic behavior of the dynamical systems [19–21]. Let the triple  $(X, f, d)$  be a flow or semi-flow. Then, the definition of unpredictability can be given as follows.

**Definition 1** ([19]). *The trajectory through a point  $p \in X$  and the point itself are unpredictable if there exists a positive number  $\Delta$  and the sequences of convergence  $t_n$  and separation  $s_n$ , both of which diverge to infinity, such that  $\lim_{n \rightarrow \infty} f(t_n, p) = p$  and  $d[f(s_n, f(t_n, p)), f(s_n, p)] \geq \Delta$  for each natural number  $n$ .*

In this definition, the distance between  $f(t_n, p)$  and the initial point  $p$  decreases for each turn  $n$  of the trajectory, or there is a recurrence, for an infinite turn. The sequence of  $t_n$  values is called the sequence of convergence. This phenomenon is called Poisson stability, which is a mandatory condition for unpredictability. If the trajectories starting from  $p$  and  $f(t_n, p)$  diverge with a distance greater than  $\Delta$  at the moments  $s_n$  such that  $d[f(s_n, f(t_n, p)), f(s_n, p)] \geq \Delta$ , then the motion is unpredictable. The sequence of  $s_n$  values is called the sequence of separation. The algorithm to numerically implement this analysis is given in the paper [18]. The presence of unpredictable trajectories indicates the existence of Poincaré chaos [19–21].

In numerical simulations, the existence and strength of unpredictability, or chaos, can be measured by the following numerical characteristic of unpredictability

$$\alpha_k = \frac{\min_{1,2,\dots,k} \delta_n}{\Delta} \tag{1}$$

for a finite number  $k$ , which is called the degree of numerical unpredictability. Here, the maximum possible distance between the initial point,  $p$ , and point  $f(t_n, p)$  is denoted by  $\delta_n$  such that  $d[p, f(t_n, p)] \leq \delta_n$ . The unpredictability is numerically approved if  $\alpha_k$  is a small number and converges to zero for large  $k$ . In the same manner, smaller  $\alpha_k$  implies stronger unpredictability.

Let the unidirectionally coupled systems be given as

$$\dot{x} = f(x), \tag{2}$$

$$\dot{y} = g(y, h(x)), \tag{3}$$

where these two systems, (2) and (3), are called drive and response systems, respectively. There are different types of methods to show the synchronization of chaos between both systems. The present study concerns the delta synchronization of chaos, and for comparison, generalized synchronization with an auxiliary system approach.

The definition of delta synchronization of chaos can be given for the unpredictable solutions  $x(t)$  and  $y(t)$  as follows.

**Definition 2** ([17,18]). *The systems (2) and (3) with unpredictable motions  $x(t)$  and  $y(t)$  admit the delta synchronization of chaos, if there exist positive numbers  $\delta, \Delta_1, \Delta_2, \delta < \Delta_{1,2}$ , the sequence of finite convergence  $u_n$  and sequence of separation  $v_n$  such that  $\|x(u_n) - x(0)\| + \|y(u_n) - y(0)\| = \delta_n \leq \delta$ ,  $\|x(u_n + v_n) - x(v_n)\| \geq \Delta_1$  and  $\|y(u_n + v_n) - y(v_n)\| \geq \Delta_2, n = 1, 2, \dots$*

The DSC method focuses on the common moments of finite converging and diverging between drive and response systems. In the case of complete converging,  $\lim_{n \rightarrow \infty} \delta_n = 0$ , the synchronization is stronger and it is called complete synchronization of unpredictability. The existence and strength of DSC can be measured by the following numerical characteristic

$$\alpha_k^{sync} = \frac{\delta_k}{\min(\Delta_1, \Delta_2)} \tag{4}$$

for non-increasing sequence  $\delta_k, n = 1, 2, \dots, k$ , which is called the degree of numerical synchronization. The DSC is approved for small numbers of  $\alpha_k^{sync}$  such that  $\alpha_k^{sync} < 1$ . The synchronization is stronger for smaller values of  $\alpha_k^{sync}$ . Moreover, it is called complete synchronization of unpredictability if  $\alpha_k^{sync} \rightarrow 0$  as  $k \rightarrow \infty$ .

One of the canonical types of chaos synchronization is generalized synchronization [4,5]. In this study, the auxiliary system approach of generalized synchronization [5] is employed for the comparison with DSC. The generalized synchronization occurs between (2) and (3) if  $I_x, I_y$  initial condition sets exist such that all  $x_0 \in I_x$  and  $y_{10}, y_{20} \in I_y$  and satisfy the following condition

$$\lim_{t \rightarrow \infty} \|y(t, x_0, y_{10}) - y(t, x_0, y_{20})\| = 0, \text{Mackey} - \text{Glass} \tag{5}$$

which is called the asymptotic stability condition. This condition is examined after the transient regime in the numerical simulations.

The particular difference between generalized synchronization and the DSC is that the former focuses on the synchronization of whole motion omitting the transient regime, but the latter only considers the moments  $u_n$  (moments of convergence) and  $v_n$  (moments of separation) to show the existence of synchronization. The advantage of delta synchronization is its capability of detecting the synchronization between chaotic drive and response systems in regimes, where generalized synchronization does not exist [17,18]. It will be shown that when generalized synchronization exists, complete synchronization of unpredictability, which is the stronger version of delta synchronization, also exists.

### 3. Transition to Chaotic Regime in Mackey–Glass System

The equation of the Mackey–Glass system is defined as follows:

$$\frac{dx}{dt} = f(x, x_\tau) \equiv \frac{ax_\tau}{1 + (x_\tau)^b} - cx, \tag{6}$$

where  $x_\tau \equiv x(t - \tau)$  indicates the time-delay variable;  $\tau, a, b, c > 0$  are real parameters and  $\tau$  represents the delay time. In this paper, we apply the Definition 1 for  $X = \mathbb{R}$ , and the distance is determined through the absolute value of real numbers.

By varying the parameters, dynamical features of the Mackey–Glass system, particularly periodic and chaotic oscillations, have been extensively investigated [30,31,35–37,39]. Different parameters in the model lead to variations in several key properties. These include the delay time  $\tau$  for the transition to chaotic regimes, the stability and oscillatory behavior of the model, the occurrence of bifurcation cascades, and the effects of perturbations applied to the system [39–42]. Here, the input parameters of Refs. [35,37] are specifically considered such that  $a, b$ , and  $c$  are fixed at 2, 10, and 1, respectively.

The transition from periodic oscillations to chaotic ones is obtained by varying the delay time  $\tau$ . Increasing  $\tau$  leads to the birth of new periods through period-doubling bifurcations and the disappearance of periodic behaviors with the transition to fully chaotic states. Such a local change in stability is known as Hopf bifurcation [43,44].

Figure 1 demonstrates the temporal oscillations of variable  $x$  at  $\tau = 1.40$  and  $\tau = 1.565$ . The point  $A$  at  $\tau = 1.40$  becomes an inflection point at  $\tau = 1.565$ . The formation of an inflection point in the waveform corresponds to the emergence of a new period along the curve  $f(x, x_\tau) = 0$  in the return map Figure 2. In order to mark the beginning of a new period formation, Figure 3 displays the results of calculations with  $\tau = 1.40, 1.456, 1.49$ , and  $1.565$ . Please note that the point  $A$  intersects the  $f(x, x_\tau) = 0$  curve at  $\tau = 1.456$ , representing the birth of a new period. At  $\tau = 1.49$  and  $\tau = 1.565$ , point  $A$  becomes the maximum of the corresponding waveform and intersects the solution of  $f(x, x_\tau) = 0$  curve with an additional intersection point, which represents the local minimum of this new periodic motion. Point  $A$  occurs when the first and second derivatives are equal to zero ( $\frac{dx}{dt} = \frac{d^2x}{dt^2} = 0$ ). This situation is shown in Figure 4. Please note that the intersection point of the first and second derivatives along the  $y$  axis corresponds to the point  $A$  of the solution  $x(t)$ .

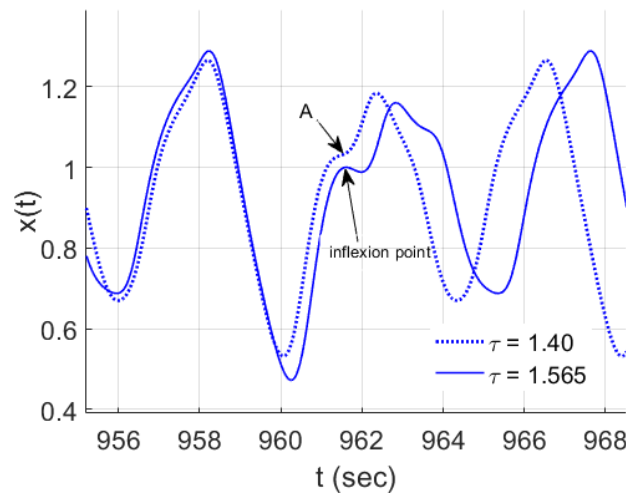


**Figure 1.** Time oscillations of variable  $x$  at  $\tau = 1.40$  and  $\tau = 1.565$ . Point  $A$  at  $\tau = 1.40$  evolves into an inflection point at  $\tau = 1.565$ .

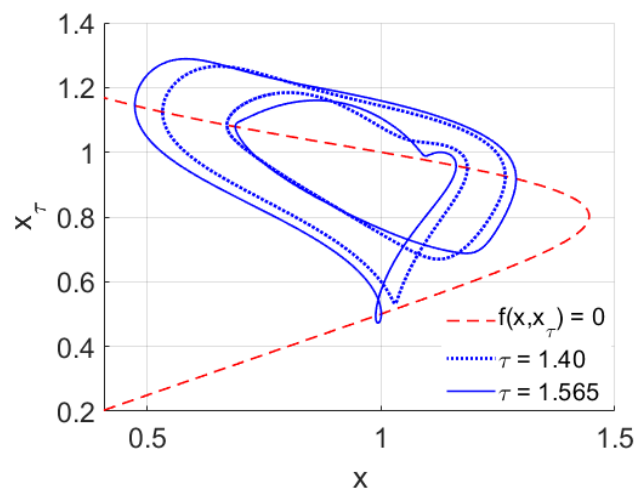


**Figure 2.** Emerging of a new period along the curve  $f(x, x_\tau) = 0$ .

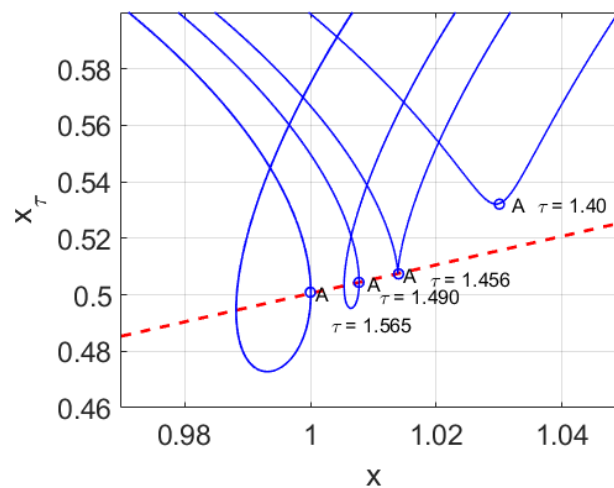


**Figure 3.** The beginning of a new period formation along the curve  $f(x, x_\tau) = 0$ . Calculations are carried out at  $\tau = 1.40, 1.456, 1.49, \text{ and } 1.565$ .

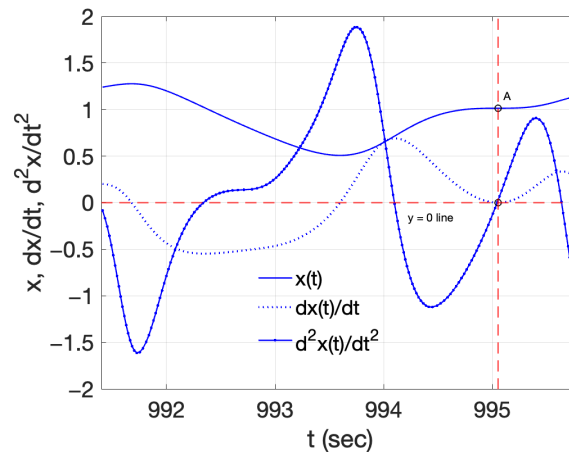


**Figure 4.** Time oscillations of  $x, \frac{dx}{dt}, \frac{d^2x}{dt^2}$ , where the intersection point of  $\frac{dx}{dt}$  and  $\frac{d^2x}{dt^2}$  along the y-axis corresponds to the point A on the solution  $x$ .

The diagram in Figure 5, which shows the onset of period-doubling bifurcation cascade in the plane of  $x(t)$  and  $\tau$ , is derived by considering local maximums (peaks) of oscillations against delay time. Please note that a single new branch begins suddenly at  $\tau = 1.475$ , and its birth depends on the chosen values of constants  $a, b$  [40–42]. Indeed, more familiar bifurcations, not including the birth and death of abruptly emerging branches, can be obtained by choosing the appropriate constant values. Different bifurcation diagrams for various  $a, b, c$  values are given in Refs. [40–42]. By varying these parameters, the system’s dynamics can undergo transitions from chaotic to periodic behavior within certain ranges of the delay time, followed by a return to chaotic regimes. This behavior is not observed with the parameters used in this paper.

The vertical lines in the bifurcation diagram, Figure 5, denote the values  $\tau = 1.2, 1.4, 1.55,$  and  $2.5$  corresponding to the regimes (a)–(d) shown in Figure 6. The transient solutions in the phase portraits (a)–(d) are excluded. In Figure 6a, the oscillations move away from fixed point  $x = 1$  and eventually develop into limit cycle oscillations with a single period. Figure 6b oscillates with two periods, and a new periodic trajectory (a third one) emerges from an existing one in Figure 6c. The period-doubling bifurcation is generally considered a typical route to temporal chaos [45,46] such that Figure 6d shows a fully chaotic state.

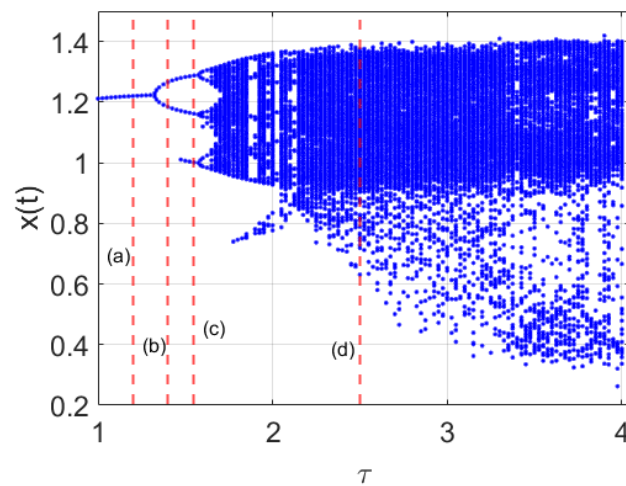


**Figure 5.** The onset of the period-doubling bifurcation cascade. The regimes (a), (b), (c), and (d) correspond to those in Figure 6.

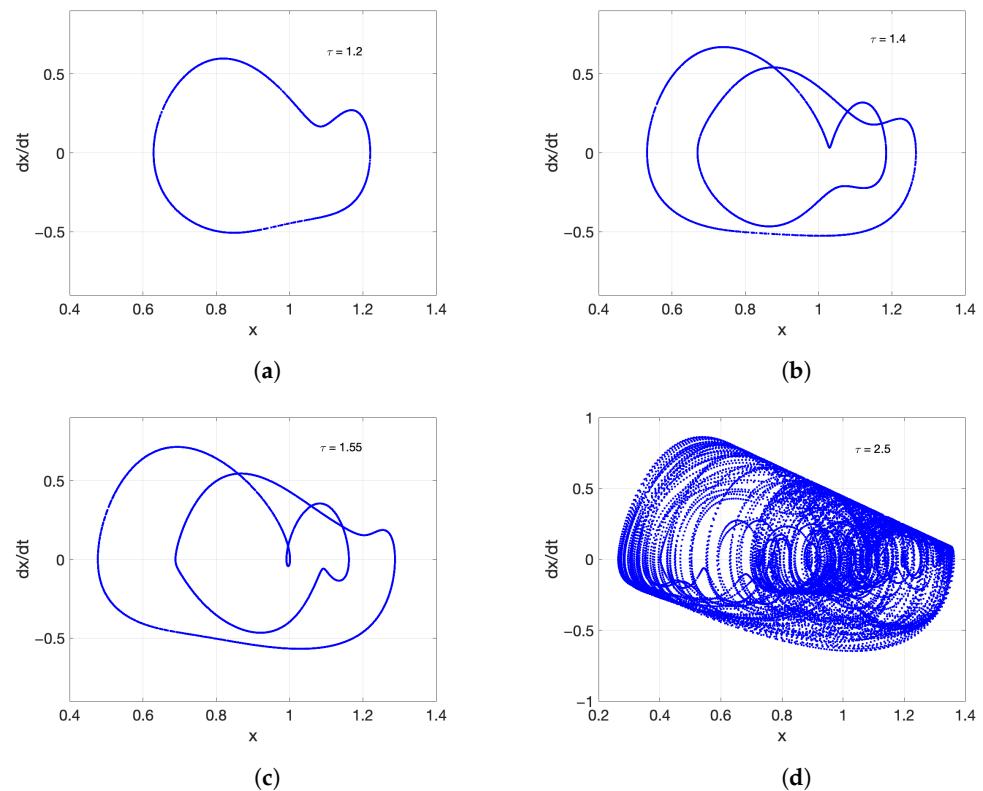


**Figure 6.** Phase space trajectories of the oscillations in the plane of  $\frac{dx}{dt}$  and  $x$  for various delay values  $\tau$  defined in Figure 5.

In Refs. [35,37], the stable and unstable oscillations are classified at the fixed point  $x = 1$  by varying  $\tau$  with the same  $a, b$ , and  $c$  values. It was concluded that the solutions are chaotic when  $\tau > 1.68$  is satisfied. In the following analysis, a fully chaotic state,  $\tau = 100$ , is considered.

#### 4. The Novel Synchronization of Chaos

The unidirectionally coupled Mackey–Glass systems with the constants in Section 3 can be given as follows

$$\frac{dx}{dt} = \frac{2x_\tau}{1 + x_\tau^{10}} - x, \tag{7a}$$

$$\frac{dy}{dt} = \frac{2y_\tau}{1 + y_\tau^{10}} - y + \varepsilon(x - y), \tag{7b}$$

where  $x_\tau \equiv x(t - \tau)$ ,  $y_\tau \equiv y(t - \tau)$  and  $\varepsilon$  is the coupling constant. Equations (7a) and (7b) are called drive and response systems, respectively. We set  $\tau = 100$  as a constant value to ensure chaotic motion [35,37].

For the analysis of generalized synchronization, the auxiliary system can be defined as follows:

$$\frac{dz}{dt} = \frac{2z_\tau}{1 + z_\tau^{10}} - z + \varepsilon(x - z). \tag{8}$$

Generalized synchronization is achieved for the drive and response systems if the asymptotic stability condition (5) is satisfied for the response and auxiliary systems.

The synchronization threshold for generalized synchronization is given in the paper [37], which is  $\varepsilon_c \approx 0.702$ . The generalized synchronization occurs above the synchronization threshold,  $\varepsilon > \varepsilon_c$ , and below the threshold,  $\varepsilon < \varepsilon_c$ , generalized synchronization is non-existent. The present study considers the two particular coupling constants for the comparison of the DSC with the generalized synchronization, such that one is above but still at the vicinity of the synchronization threshold,  $\varepsilon = 0.71$ , and the other is below and relatively smaller than the threshold, which is  $\varepsilon = 0.6$ .

The unpredictability and DSC analyses in both regions consider the simulation time  $t_{sim} = 500,000$  with the time difference  $\Delta t = 0.2$ . The drive and response systems also have the same  $t_{sim}$  and  $\Delta t$  for consistency.

#### 4.1. Synchronization of Chaos above the Threshold

Let  $\varepsilon = 0.71$  for the coupled systems (7a) and (7b). Generalized synchronization between these systems is approved by utilizing the auxiliary system (8) as shown in Figure 7. The figure demonstrates that the motion takes place on the  $y = z$  line; hence, the asymptotic stability condition (5) is satisfied. The transient regime is discarded in the analysis.

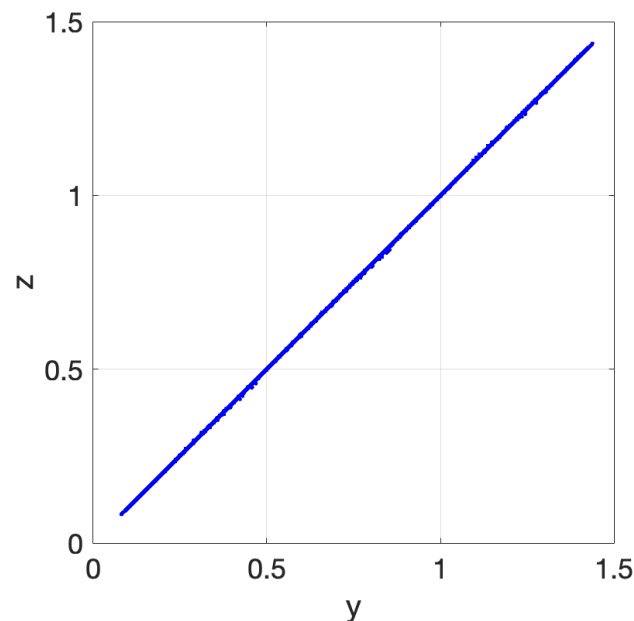
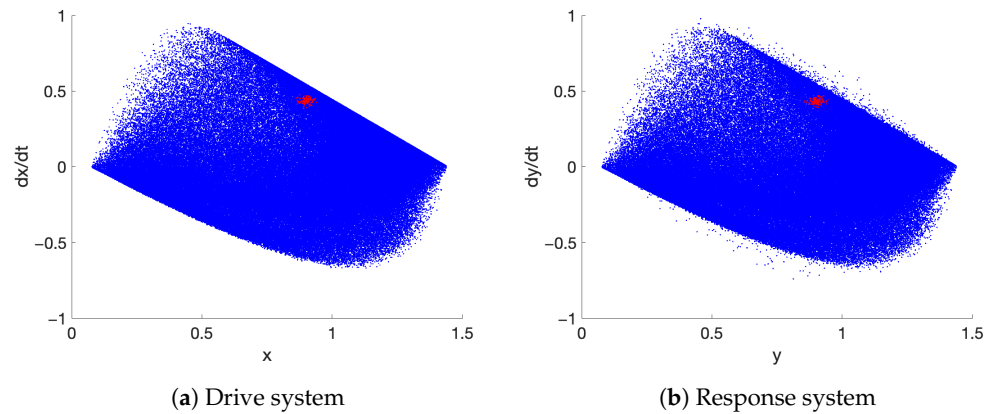


Figure 7. Projection of response and auxiliary systems on  $(y, z)$  plane for  $\varepsilon = 0.71$  after transient regime.

In the unpredictability analysis, we take  $\Delta_d = 1.4$  and  $\Delta_r = 1.19$  for the drive and response systems, respectively. The values of  $\delta$  become smaller for each member of sequences of convergence and separation as  $\delta_1 = 0.0500, \delta_2 = 0.0497, \delta_3 = 0.0494, \dots$ . The phase portraits of drive and response systems are demonstrated in Figure 8, where the red marks represent  $(x(t_n), \dot{x}(t_n))$  and  $(y(t_n), \dot{y}(t_n))$  for Figure 8a,b, respectively.



**Figure 8.** Phase portraits of drive and response systems for  $\varepsilon = 0.71$ . Red marks represent  $(x(t_n), \dot{x}(t_n))$  and  $(y(t_n), \dot{y}(t_n))$ .

The unpredictable motion in the drive system is presented by Table 1, which demonstrates the sequences of convergence and divergence, and  $\delta_n$  values. There are 163  $t_n$  and  $s_n$  values with the  $\delta_{163} = 0.0014$ . The degree of numerical unpredictability is  $\alpha_{163} = 0.0014/1.4 = 0.001$ , which is a small number obtained in the large simulation time  $t_{sim} = 500,000$ . Thus, unpredictability in the drive system is approved by the conditions of Definition 1.

**Table 1.** Sequences of convergence  $t_n$  and divergence  $s_n$  with  $\delta_n$  values for the drive system.

$n$	$t_n$	$s_n$	$\delta_n$
1	1006	1420	0.0500
2	1017	2332	0.0497
3	1114	3401	0.0494
4	1409	3667	0.0491
5	1606	4384	0.0488
	⋮		
	⋮		
159	126,954	139,195	0.0026
160	182,244	139,343	0.0023
161	211,316	141,346	0.0020
162	216,785	141,724	0.0017
163	307,457	141,799	0.0014

The unpredictable motion of the response system is presented in Table 2. The sequences of convergence and divergence have 165 time moments. For the large simulation time  $t_{sim} = 500,000$ , the smallest distance between the trajectories and the initial point is  $\delta_{165} = 0.0008$ . The degree of unpredictability,  $\alpha_{165} = 0.0008/1.19 \approx 0.0007$ , is a sufficiently small number demonstrating the chaotic nature of the motion. Thus, the unpredictable behavior of the response system is approved based on Definition 1.

**Table 2.** Sequences of convergence  $t_n$  and divergence  $s_n$  with  $\delta_n$  values for the response system for  $\varepsilon = 0.71$ .

$n$	$t_n$	$s_n$	$\delta_n$
1	1006	110	0.0500
2	1017	197	0.0497
3	1114	713	0.0494
4	1409	832	0.0491
5	1606	833	0.0488
	⋮		
	⋮		
161	126,235	13,408	0.0020
162	126,954	13,416	0.0017
163	182,244	13,440	0.0014
164	183,663	13,502	0.0011
165	486,244	13,587	0.0008

The common sequences of convergence  $u_n$  and divergence  $v_n$  based on the conditions given in Definition 2 are presented in Table 3. The sequences of convergence  $u_n$  and divergence  $v_n$  have 155 and 151 time moments, respectively. For the largest  $v_n$  value,  $\delta_n = 0.005$ , which is a small number for the simulation time  $t_{sim} = 500,000$ . In the simulation time, the separation moments for  $n = 152, 153, 154$ , and 155 are not detected. It is important to note that prolonging the simulation further to detect more  $v_n$  moments is not necessary for two reasons. First, the 151 elements in the sequence of separation are sufficiently close to the length of the sequences in the drive and response systems, which are 163 and 165, respectively. Second,  $\delta_{151} = 0.005$  is a sufficiently small number for the synchronization analysis. Hence, the complete synchronization of unpredictability is approved by the degree of numerical synchronization  $\alpha_{151}^{synch} = 0.0036$ .

**Table 3.** Common sequences of convergence  $u_n$  and divergence  $v_n$  with  $\delta_n$  between drive and response systems  $\varepsilon = 0.71$ .

$n$	$u_n$	$v_n$	$\delta_n$
1	1006	3607	0.0500
2	1017	3913	0.0497
3	1738	4369	0.0494
	⋮		
	⋮		
145	216,785	181,017	0.0068
146	216,959	181,879	0.0065
147	235,239	182,025	0.0062
148	254,539	182,691	0.0059
149	282,905	183,994	0.0056
150	302,035	185,132	0.0053
151	307,457	187,115	0.0050
152	312,688	-	0.0047
153	343,333	-	0.0044
154	362,248	-	0.0041
155	486,244	-	0.0038

It is shown that the generalized synchronization and complete synchronization of unpredictability coexist above the synchronization threshold. The coupling  $\varepsilon = 0.71$  is chosen near the threshold  $\varepsilon_c \approx 0.702$  since increasing this value makes the synchronization stronger and already implies the coexistence of both synchronizations.

#### 4.2. Synchronization of Chaos below the Threshold

For the coupled systems (7a) and (7b), synchronization of the chaos below the threshold is considered at  $\epsilon = 0.60$ . Utilization of the auxiliary system (8) enables us to show that the coupled systems have no generalized synchronization at  $\epsilon = 0.60$  as can be seen in Figure 9. The figure demonstrates that the motion does not take place on the  $y = z$  line. Therefore, the asymptotic stability condition (5) is not satisfied and the absence of the generalized synchronization is confirmed.

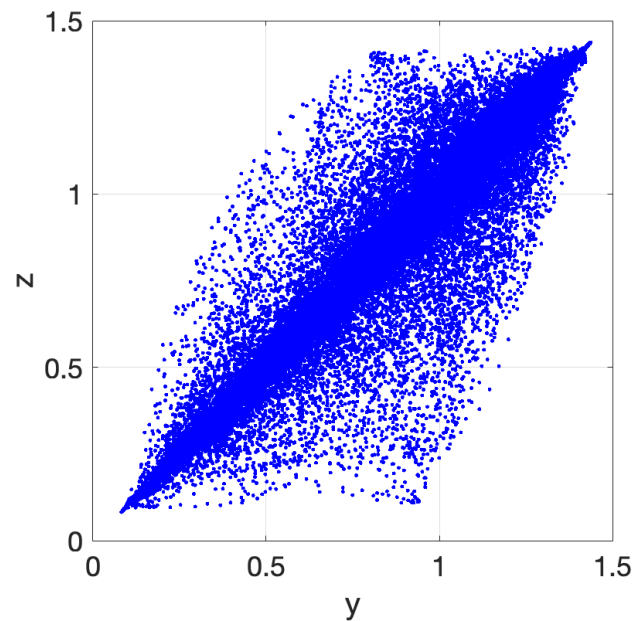


**Figure 9.** Projection of response and auxiliary systems on  $(y, z)$  plane for  $\epsilon = 0.60$  after transient regime.

The unpredictability analysis is implemented to the response system with new coupling  $\epsilon = 0.60$  for  $\Delta_r = 1.42$ . The distance between the initial point and  $y(t_n)$  takes the values  $\delta_1 = 0.0500, \delta_2 = 0.0497, \delta_3 = 0.0494, \dots$  as before. The phase portrait of the response system  $(y(t_n), \dot{y}(t_n))$  represented by red marks is given in Figure 10. Since the coupling  $\epsilon$  is not present in the drive system, it is exactly the same as in Section 4.1. Therefore, the phase portrait and table of unpredictability, given in the previous subsection as Figure 8a and Table 1, are still valid for the analysis of this subsection. Let us also emphasize that the only difference between the response system here and in Section 4.1 is the coupling constant.

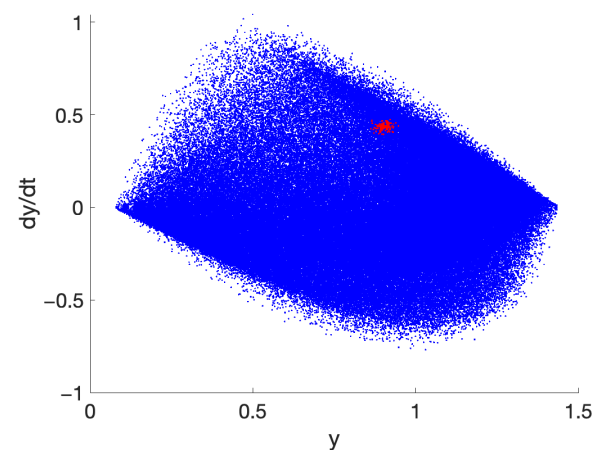


**Figure 10.** Phase portrait of the response system for  $\epsilon = 0.6$ . Red marks represent  $(y(t_n), \dot{y}(t_n))$ .

The sequences of convergence and divergence with the  $\delta_n$  values in the response system are presented in Table 4. The sequences include 165 time moments with the final distance  $\delta_{165} = 0.0008$  between  $y(0)$  and  $y(t_{165})$ . The numerical characteristic of the unpredictable motion, degree of numerical unpredictability  $\alpha_{165} \approx 0.0006$ , is a sufficiently small number obtained within the large simulation time  $t_{sim} = 500,000$ . Thus, the unpredictability is approved by the terms of Definition 1.

**Table 4.** Sequences of convergence  $t_n$  and divergence  $s_n$  with  $\delta_n$  values for the response system  $\varepsilon = 0.60$ .

$n$	$t_n$	$s_n$	$\delta_n$
1	1006	2823	0.0500
2	1017	3306	0.0497
3	1111	3340	0.0494
4	1409	3667	0.0491
5	1606	4384	0.0488
	⋮		
	⋮		
161	188,812	178,538	0.0020
162	219,069	179,205	0.0017
163	235,464	179,861	0.0014
164	238,264	180,461	0.0011
165	301,502	180,473	0.0008

The common sequences of finite convergence and divergence, described in Definition 2, are given in Table 5. Although there are 132  $u_n$  values in the sequence of finite convergence, any common time moment is not detected after  $v_{108}$  for the sequence of separation. The smallest relevant distance  $\delta_n$  is  $\delta_{108} = 0.0179$ , which is relatively large compared to the previous unpredictability and complete synchronization of unpredictability analyses. The degree of numerical synchronization is  $\alpha_{108}^{synch} = 0.013$ , which is 3.6 times larger than the degree of numerical synchronization for the analysis above the threshold and yet smaller than one. Hence, delta synchronization of chaos is approved by Definition 2.

**Table 5.** Common sequences of convergence  $u_n$  and divergence  $v_n$  with  $\delta_n$  between drive and response systems  $\varepsilon = 0.60$ .

$n$	$u_n$	$v_n$	$\delta_n$
1	1017	2332	0.0500
2	1738	2389	0.0497
3	1938	3710	0.0494
	⋮		
	⋮		
105	159,340	310,116	0.0188
106	167,894	311,753	0.0185
107	169,829	312,105	0.0182
108	172,648	314,333	0.0179
109	188,812	-	0.0176
	⋮		
	⋮		
132	497,535	-	0.0107

For  $\varepsilon = 0.60$ , which is below the synchronization threshold  $\varepsilon \approx 0.702$  given for generalized synchronization analysis with the specified parameters [37], the delta synchronization of chaos is detected in the absence of generalized synchronization.

Previous analyses in the literature, such as in [35,37], examined chaos synchronization and found the critical coupling value for the occurrence of the phenomenon in the Mackey–Glass system. The present study reproduced the results of Ref. [37] above the threshold and illustrated the coexistence of generalized synchronization and complete synchronization of unpredictability. While existing literature predominantly focuses on synchronization types above the threshold [33,35–38], our research demonstrates the existence of this phenomenon and its detection using the DSC method below the threshold. Thus, on both sides of the threshold, the synchronization of chaos through unpredictability is verified.

## 5. Conclusions

In this study, we explored the synchronization of chaos in Mackey–Glass time-delay systems. By analyzing the unpredictability of the drive and response systems, we confirmed the existence of chaos in both. The synchronization phenomenon has been revealed through the application of the novel DSC method, which is based on the analysis of unpredictability. The primary novelty of our study resides in revealing the synchronization phenomenon in a domain that was previously proven unattainable for conservative methods [37]. Specifically, we discovered the synchronization of chaotic systems for a coupling constant below the conventional synchronization threshold.

By varying the coupling constant beyond the synchronization threshold in unidirectionally coupled Mackey–Glass systems, we observed changes in the synchronization characteristics of the model. Above the synchronization threshold, we found the coexistence of generalized synchronization and complete synchronization of unpredictability. Notably, even when the coupling is close to the threshold but still greater, the DSC analysis detected the presence of complete synchronization of unpredictability.

However, our main result lies in the analysis below the synchronization threshold, where generalized synchronization is absent. In this region, we have demonstrated the existence of delta synchronization of chaos, a novel form of synchronization analyzing time sequences of the model. Thus, the threshold is no longer a requirement for the synchronization of chaos through unpredictability. These findings are consistent with similar results found in different models, as reported in Refs. [17,18], suggesting that the DSC method can reveal the synchronization phenomenon in the absence of generalized synchronization. Nevertheless, the presence of a boundary for achieving synchronization through unpredictability remains an open problem.

To support our analyses and results, we provided specific numerical characteristics of unpredictability and DSC, along with relevant tables presenting the time sequences of convergence and separation. Based on the degree of numerical unpredictability, both the drive and response systems exhibit unpredictable behavior for all coupling constants. Above the threshold, we observed a strong degree of numerical synchronization, corroborating the presence of complete synchronization of unpredictability. Mainly, below the threshold, the numerical characteristic exhibits a significant increase, indicating weaker synchronization, which confirms the existence of delta synchronization of chaos.

**Author Contributions:** Conceptualization, M.A., K.B. and C.Y.; methodology, M.A.; software, K.B. and C.Y.; validation, M.A., K.B. and C.Y.; formal analysis, K.B. and C.Y.; investigation, M.A., K.B. and C.Y.; resources, M.A., K.B. and C.Y.; data curation, K.B. and C.Y.; writing—original draft preparation, M.A., K.B. and C.Y.; writing—review and editing, M.A., K.B. and C.Y.; visualization, M.A., K.B. and C.Y.; supervision, M.A.; project administration, M.A. All authors have read and agreed to the published version of the manuscript.

**Funding:** M. Akhmet and K. Başkan have been supported by 2247-A National Leading Research Program of TÜBİTAK (The Scientific and Technological Research Council of Turkey), Turkey, N 120C138.

**Data Availability Statement:** The data presented in this study are only available in the current paper.

**Acknowledgments:** The authors wish to express their sincere gratitude to the referees for the helpful criticism and valuable suggestions, which helped to improve the paper significantly.

**Conflicts of Interest:** The authors declare no conflict of interest.

## References

1. Pecora, L.M.; Carroll, T.L. Driving systems with chaotic signals. *Phys. Rev. A* **1991**, *44*, 2374. [[CrossRef](#)]
2. Ogorzalek, M.J. Taming Chaos-Part I: Synchronization. *IEEE Trans. Circuits Syst. Fundam. Theory Appl.* **1993**, *40*, 693–699. [[CrossRef](#)]
3. Rulkov, N.F.; Sushchik, M.M.; Tsimring, L.S.; Abarbanel, H.D. Generalized synchronization of chaos in directionally coupled chaotic systems. *Phys. Rev. E* **1995**, *51*, 980. [[CrossRef](#)] [[PubMed](#)]
4. Kocarev, L.; Parlitz, U. Generalized synchronization, predictability, and equivalence of unidirectionally coupled dynamical systems. *Phys. Rev. Lett.* **1996**, *76*, 1816. [[CrossRef](#)]
5. Abarbanel, H.D.; Rulkov, N.F.; Sushchik, M.M. Generalized synchronization of chaos: The auxiliary system approach. *Phys. Rev. E* **1996**, *53*, 4528. [[CrossRef](#)] [[PubMed](#)]
6. Pyragas, K. Weak and strong synchronization of chaos. *Phys. Rev. E* **1996**, *54*, R4508. [[CrossRef](#)] [[PubMed](#)]
7. Min, F.; Ma, H. The mechanism of switching combination synchronization for three distinct nonautonomous systems under sinusoidal constraints. *Nonlinear Dyn.* **2020**, *100*, 475–492. [[CrossRef](#)]
8. Min, F.; Luo, A.C. Complex dynamics of projective synchronization of Chua circuits with different scrolls. *Int. J. Bifurc. Chaos* **2015**, *25*, 1530016. [[CrossRef](#)]
9. Ma, J.; Mi, L.; Zhou, P.; Xu, Y.; Hayat, T. Phase synchronization between two neurons induced by coupling of electromagnetic field. *Appl. Math. Comput.* **2017**, *307*, 321–328. [[CrossRef](#)]
10. Nana, B.; Woafu, P.; Domngang, S. Chaotic synchronization with experimental application to secure communications. *Commun. Nonlinear Sci. Numer. Simul.* **2009**, *14*, 2266–2276. [[CrossRef](#)]
11. Heil, T.; Fischer, I.; Elsässer, W.; Mulet, J.; Mirasso, C.R. Chaos synchronization and spontaneous symmetry-breaking in symmetrically delay-coupled semiconductor lasers. *Phys. Rev. Lett.* **2001**, *86*, 795. [[CrossRef](#)] [[PubMed](#)]
12. Wang, S.; Shi, K. Mixed-Delay-Dependent Augmented Functional for Synchronization of Uncertain Neutral-Type Neural Networks with Sampled-Data Control. *Mathematics* **2023**, *11*, 872. [[CrossRef](#)]
13. Li, M.; Fan, Y. Aperiodic Sampled-Data Control for Anti-Synchronization of Chaotic Nonlinear Systems Subject to Input Saturation. *Axioms* **2023**, *12*, 403. [[CrossRef](#)]
14. Caneco, A.; Grácio, C.; Rocha, J.L. Kneading theory analysis of the Duffing equation. *Chaos Solitons Fractals* **2009**, *42*, 1529–1538. [[CrossRef](#)]
15. González-Miranda, J.M. *Synchronization and Control of Chaos*; Imperial College Press: London, UK, 2004.
16. Pikovsky, A.; Rosenblum, M.; Kurths, J. *Synchronization, A Universal Concept in Nonlinear Sciences*; Cambridge University Press: Cambridge, UK, 2001.
17. Akhmet, M.; Başkan, K.; Yeşil, C. Delta synchronization of Poincaré chaos in gas discharge-semiconductor systems. *Chaos Interdiscip. J. Nonlinear Sci.* **2022**, *32*, 083137. [[CrossRef](#)]
18. Akhmet, M.; Yeşil, C.; Başkan, K. Synchronization of chaos in semiconductor gas discharge model with local mean energy approximation. *Chaos Solitons Fractals* **2023**, *167*, 113035. [[CrossRef](#)]
19. Akhmet, M.; Fen, M.O. Unpredictable points and chaos. *Commun. Nonlinear Sci. Numer. Simul.* **2016**, *40*, 1–5. [[CrossRef](#)]
20. Akhmet, M.; Fen, M.O.; Alejaily, E.M. *Dynamics with Chaos and Fractals*; Springer: Cham, Switzerland, 2020.
21. Akhmet, M. *Domain Structured Dynamics: Unpredictability, Chaos, Randomness, Fractals, Differential Equations and Neural Networks*; IOP Publishing: Bristol, UK, 2021.
22. Poincaré, H. Sur le problème des trois corps et les équations de la dynamique. *Acta Math.* **1890**, *13*, A3–A270.
23. Carathéodory, C. *Über den Wiederkehrsatz von Poincaré*; Springer: Berlin/Heidelberg, Germany, 1919; pp. 580–584.
24. Zhang, T.; Li, Y. Exponential Euler scheme of multi-delay Caputo–Fabrizio fractional-order differential equations. *Appl. Math. Lett.* **2022**, *124*, 107709. [[CrossRef](#)]
25. Fen, F.T.; Fen, M.O.; Akhmet, M. A novel criterion for unpredictable motions. *Filomat* **2023**, *37*, 6149–6158.
26. Akhmet, M.; Tleubergenova, M.; Zhamanshin, A. Compartmental Unpredictable Functions. *Mathematics* **2023**, *11*, 1069. [[CrossRef](#)]
27. Kinzel, W.; Englert, A.; Kanter, I. On chaos synchronization and secure communication. *Philos. Trans. R. Soc. A Math. Phys. Eng. Sci.* **2010**, *368*, 379–389. [[CrossRef](#)] [[PubMed](#)]
28. Li, D.; Wang, Z.; Zhou, J.; Ni, J.; Fang, J. A note on chaotic synchronization of time-delay secure communication systems. *Chaos Solitons Fractals* **2008**, *38*, 1217–1224. [[CrossRef](#)]
29. Kwon, O.; Park, J.H.; Lee, S. Secure communication based on chaotic synchronization via interval time-varying delay feedback control. *Nonlinear Dyn.* **2011**, *63*, 239–252. [[CrossRef](#)]
30. Mackey, M.C.; Glass, L. Oscillation and chaos in physiological control systems. *Science* **1977**, *197*, 287–289. [[CrossRef](#)]
31. Farmer, J.D. Chaotic attractors of an infinite-dimensional dynamical system. *Phys. D Nonlinear Phenom.* **1982**, *4*, 366–393. [[CrossRef](#)]
32. Namajūnas, A.; Pyragas, K.; Tamaševičius, A. An electronic analog of the Mackey–Glass system. *Phys. Lett. A* **1995**, *201*, 42–46. [[CrossRef](#)]
33. Kittel, A.; Parisi, J.; Pyragas, K. Generalized synchronization of chaos in electronic circuit experiments. *Phys. D Nonlinear Phenom.* **1998**, *112*, 459–471. [[CrossRef](#)]

34. Sano, S.; Uchida, A.; Yoshimori, S.; Roy, R. Dual synchronization of chaos in Mackey–Glass electronic circuits with time-delayed feedback. *Phys. Rev. E* **2007**, *75*, 016207. [[CrossRef](#)]
35. Dong, L.; Zhi-Gang, Z. Multiple attractors and generalized synchronization in delayed Mackey–Glass systems. *Chin. Phys. B* **2008**, *17*, 4009. [[CrossRef](#)]
36. Pyragas, K. Synchronization of coupled time-delay systems: Analytical estimations. *Phys. Rev. E* **1998**, *58*, 3067. [[CrossRef](#)]
37. Zhan, M.; Wang, X.; Gong, X.; Wei, G.; Lai, C.H. Complete synchronization and generalized synchronization of one-way coupled time-delay systems. *Phys. Rev. E* **2003**, *68*, 036208. [[CrossRef](#)] [[PubMed](#)]
38. Shahverdiev, E.; Nuriev, R.; Hashimov, R.; Shore, K. Chaos synchronization between the Mackey–Glass systems with multiple time delays. *Chaos Solitons Fractals* **2006**, *29*, 854–861. [[CrossRef](#)]
39. Junges, L.; Gallas, J.A. Intricate routes to chaos in the Mackey–Glass delayed feedback system. *Phys. Lett. A* **2012**, *376*, 2109–2116. [[CrossRef](#)]
40. Tarigo, J.P.; Stari, C.; Cabeza, C.; Marti, A.C. Characterizing multistability regions in the parameter space of the Mackey–Glass delayed system. *Eur. Phys. J. Spec. Top.* **2022**, *231*, 273–281. [[CrossRef](#)]
41. Li, L. Bifurcation and chaos in a discrete physiological control system. *Appl. Math. Comput.* **2015**, *252*, 397–404. [[CrossRef](#)]
42. El-Sayed, A.; Salman, S.; Elabd, N. On the dynamics of the singularly perturbed Mackey–Glass equation. *J. Comput. Appl. Math.* **2018**, *344*, 154–160. [[CrossRef](#)]
43. Wei, J. Bifurcation analysis in a scalar delay differential equation. *Nonlinearity* **2007**, *20*, 2483. [[CrossRef](#)]
44. Wan, A.; Wei, J. Bifurcation analysis of Mackey–Glass electronic circuits model with delayed feedback. *Nonlinear Dyn.* **2009**, *57*, 85–96. [[CrossRef](#)]
45. Jackson, E.A. *Perspectives of Nonlinear Dynamics*; CUP Archive: Cambridge, UK, 1989; Volume 1.
46. Ott, E. *Chaos in Dynamical Systems*; Cambridge University Press: Cambridge, UK, 2002.

**Disclaimer/Publisher’s Note:** The statements, opinions and data contained in all publications are solely those of the individual author(s) and contributor(s) and not of MDPI and/or the editor(s). MDPI and/or the editor(s) disclaim responsibility for any injury to people or property resulting from any ideas, methods, instructions or products referred to in the content.